Journal of Combinatorial Mathematics and Combinatorial Computing, 120: 155–167
DOI:10.61091/jcmcc120-013
http://www.combinatorialpress.com/jcmcc
Received 28 June 2023, Accepted 3 April 2024, Published 30 June 2024

Combinatorial Press

Article

Stability Analysis of Tunnel Rock Mechanical Parameters Based on Multi-Source Sensor Data Fusion

Chengli Luo[1,2], Lili Liu[3,4,*], Suypan Hussin[4], and Yan Luo[5]

[1] School of Management, Suzhou University, Suzhou 234000, Anhui, China
[2] Faculty of Enfineering, National University of Singapore, Singapore 119077, Singapore
[3] Faculty of Education, Universiti Kebangsaan Malaysia, Selangor 43600, Malaysia
[4] School of Literature and Media, Suzhou University, Suzhou 234000, Anhui, China
[5] School of Civil, Environmental, and Architectural Engineering, Korea University, Seoul 136701, Korea

* **Correspondence:** shanni0312@163.com

Abstract: In this paper, the sensor is applied to the collection of rock parameter data. Aiming at the classification and evaluation of stability (i.e. rock quality), an attribute recognition model for the classification and evaluation of surrounding rock quality of underground engineering is established. Using multi-source data fusion and orthogonal numerical simulation test methods, the effects of rock mechanics parameters on the horizontal convergence of the tunnel, the settlement of the vault and the plastic zone coefficient are studied. Six factors (elastic modulus, Poisson's ratio, internal friction angle, tensile strength, cohesion and density) and three levels of orthogonal experimental solutions were selected. The method of defining similar weight by using similar number to determine the weight of evaluation index, so as to calculate the comprehensive attribute measure, and apply confidence criteria to identify the stability of rock samples. Through the analysis and evaluation of rock mass quality classification of underground engineering, the application of the model and the evaluation method of rock mass quality classification are explained. The test results match the orthogonal test results; Considering the stability of tunnel envelope, the horizontal convergence, vault settlement and plastic zone coefficient after excavation should be comprehensively considered.

Keywords: Rock mechanics, Rock mass classification, Property mathematics, Property measure function

1. Introduction

With the development of the global economy, more and more tunnels are being built in different regions and the number of problems encountered is bound to increase [1,2]. Scholars have conducted numerous studies on the stability of tunnel envelopes. [3–5] used numerical methods to carry out studies on the influence of envelope stability under different ground stress releases and concluded that the larger the ground stress release, the smaller the load borne by the anchors and the wider the development of the plastic zone of the envelope [6]. The strain measurement technique was also used to measure the strain values at key parts of the tunnel and to analyse the stress variation law of the surrounding rock body [7–10]. The equivalent elastic modulus and equivalent lateral pressure

coefficient of this type of surrounding rock after initial support were obtained by using the positive inverse analysis method.

Therefore, using existing research methods to analyse the influence of various factors on tunnel deformation and damage is of positive significance in improving the understanding of the deformation and damage mechanism of tunnel envelope pressure and the support mechanism of anchor rods, anchor cables and grouting. Due to the different degrees of non-homogeneity, anisotropy and development of joints in the surrounding rock, the stability of the tunnel envelope is closely related to the rock structure of the tunnel envelope, in addition to the tectonic and geological environment of the project area, the degree of burial and the mechanical parameters of the rock body [11]. In the process of tunnel rock stability analysis, the surrounding rock is not only the main body of the underground engineering body bearing structure, but also the main source of structural load, and the rock structure has an important influence on the characteristics of the secondary stress field distribution after excavation, the plastic zone of the surrounding rock, the support structure and the surrounding rock pressure, etc. Therefore, in the actual tunnel construction process, it is important to be able to accurately determine the structural characteristics of the surrounding rock and to classify them.

In the actual construction of tunnels, the ability to accurately determine the structural characteristics of the surrounding rock and classify them is a prerequisite and basis for the classification of the rock, the determination of the support structure parameters and the selection of the construction method [12]. In [13], by discussing the significance of rock structure and stability, structural stability and methods for finding ultimate loads, geotechnical material ontological relationships and geotechnical stability, and by combining the redundant force reinforcement method of finite element analysis, the energy criterion of non-linear stability analysis and the principle of structural stability potential energy, the method of finding ultimate loads, which is different from structural instability and material instability, is proposed and is particularly applicable to the field of complex structures, and in [14] took the physical and mechanical properties of rock structure surface and engineering geological rock group as the starting point, studied the special rock structure of tunnel envelope, and pointed out that the rock structure characteristics of tunnel envelope are mainly controlled by the tectonic extrusion fracture zone intersecting the tunnel axis at a small angle and the rock group with alternating hard and soft outputs, and concluded that the deformation and damage of tunnel envelope is mainly controlled by the rock structure. The results of this study are presented as a reference for the classification, design and construction of tunnel rock support structures in areas with complex engineering geological conditions; [15, 16] by numerically simulating the structural surface network of the tunnel rock envelope and combining the structural characteristics of the rock mass, the ANSYS finite element analysis software is used to analyse and evaluate the displacement and stress fields in the initial state of the rock envelope, during excavation and after support in three cases, and thus this provides a strong basis for validating the support method for the tunnel rock [17, 18].

2. Numerical Modeling of Tunnels

2.1. Computational Modelling

The analysis of tunnelling problems using finite element procedures requires a combination of calculation volume and accuracy. Theoretical and practical evidence shows that the stress distribution after excavation does not exceed 10 times the radius of the tunnel. Taking into account the specific engineering reality, the numerical model chosen for the calculation of the grade 3 surrounding rock is as follows: the lower part is taken to 80m below the bottom of the tunnel, the left and right side boundaries are taken to 60m outside the tunnel, the upper part is taken to 60m according to the actual burial depth of the tunnel, both sides are horizontally constrained, the bottom is vertically constrained, the analytical model is shown in Figure 1.

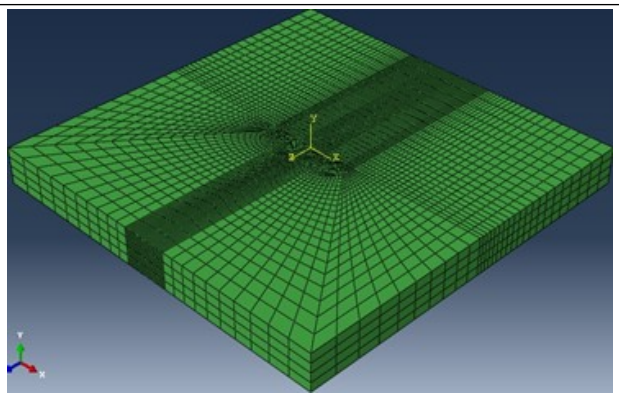

Figure 1. Model Meshing Diagram

2.2. Ontological Relations

According to the engineering geomechanical properties of the rock mass, the Mohr-Coulomb strength damage criterion was adopted. The Mohr-Coulomb ideal elastoplastic model is used for the material model of the surrounding rock, solid units are used for the surrounding rock and initial support, and the initial ground stress of the surrounding rock is simulated by considering the self-weight stress to reach equilibrium, and the Mohr-Coulomb equal area circular yielding criterion is used for the calculation, which is expressed in Eq. (1).

$$F = \partial I_1 + \sqrt{J_2} = k, \tag{1}$$

where, I_1 and J_2 are the first invariant of the stress tensor and the second invariant of the stress deflection tensor, respectively.

$$I_1 = \sigma_1 + \sigma_2 + \sigma_3. \tag{2}$$

$$J_2 = \frac{1}{3}\left[(\sigma_1 - \sigma_2) + (\sigma_2 - \sigma_3) + (\sigma_3 - \sigma_1)\right]. \tag{3}$$

Here, α and k are constants related to the angle of internal friction ϕ and cohesion C of the geotechnical material, α, k satisfying the following relations, see Eq. (4) and Eq. (5).

$$\alpha = \frac{2\sqrt{3}\sin\phi}{\sqrt{2\sqrt{3}\pi\left(9 - \sin^2\phi\right)}}, \tag{4}$$

$$k = \frac{6\sqrt{3}C\sin\phi}{\sqrt{2\sqrt{3}\pi\left(9 - \sin^2\phi\right)}}. \tag{5}$$

2.3. Selection of Engineering Mechanics Parameters

According to the engineering rock mechanical parameters obtained, the rock physical and mechanical parameters of the surrounding rock at different levels were obtained.

The specific parameters are shown in Table 1.

Index/ lithology	Severe(g/ cm^3)	Compressive strength(Mpa)	Modulus of elasticity (GPa)	Cohesion (MPa)	Internal friction angle(°)	Poisson's ratio
Granite	2.6	65.1	50.2	25.3	40.5	0.22
Granodiorite	2.6	43.5	33.2	21.5	37.7	0.19
limestone	2.6	38.8	28.2	20.3	32.9	0.18
Dolomite	2.6	35	27.6	18.4	28.7	0.18
Tuff	2.5	32.9	32.9	18.5	26.3	0.17

Table 1. Table of Physical and Mechanical Parameters of the Surrounding Rock

2.4. Numerical Simulation Process for Tunnel Excavation

The common methods of tunnel excavation are full section excavation, step excavation and step-by-step excavation. ABAQUS finite element software is very convenient for simulating the tunneling method of step-by-step construction excavation.

1. **Earth stress balance**
   The initial stress is the initial stress in the tunnel rock, which largely influences the stability of the tunnel excavation. In tunnel excavation, the influence of the initial stress field needs to be considered first, and a ground stress balance must be established when the tunnel excavation is simulated numerically.
   After the ground stress balance has been established, the tunnel excavation needs to be simulated in steps, the following is the excavation process from Grade II to Grade V surrounding rocks.
2. **Class II Rock**
   The Class II rock is a hard rock with a simple rock cover and a relatively homogeneous rock quality, so the full section blasting method was used. The tunnel excavation sequence is shown in Figure 2.

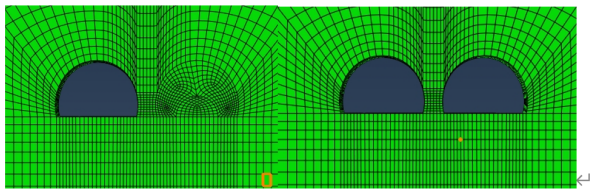

Figure 2. Construction Process Diagram for Class II Rock Surrounds

3. **Grade III Surrounding Rock**
   The rocks are slightly weathered, generally influenced by geological formations, with slightly developed joints and fissures and a blocky structure. The structural surface combination is basically stable. It is a basic stable rock, so the up and down step method is used. The specific sequence of tunnel excavation is shown in Figure 3.

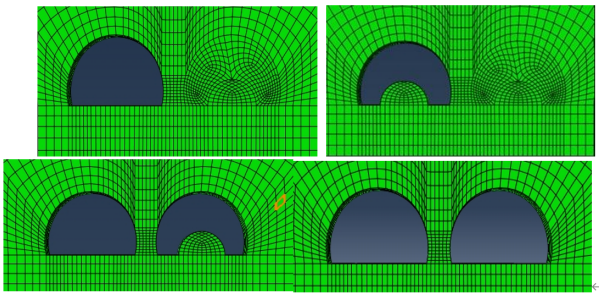

Figure 3. Construction Process Diagram for Class III Rock Surround

4. **Grade IV Surrounding Rocks**
   Grade IV surrounding rocks have more distribution of soft and weak structural surfaces, joint fissures are locally extremely developed, and the rocks have a rubble-like mosaic structure and a rubble-like crushed structure locally. This is a poorly stable rock, so a combination of up and down steps and positive sidewall guide pits is used. The tunnel excavation sequence is shown in Figure 4.
5. **Grade V Rock**
   The Grade V surrounding rocks are strongly weathered or fully weathered rocks, severely affected by geological structures, with extremely developed joints and fissures, fault fracture zones greater than 2m in width and fissures filled with mud. The rock is extremely unstable, so a combination of up and down steps and positive sidewall guide pits is used. The tunnel excavation

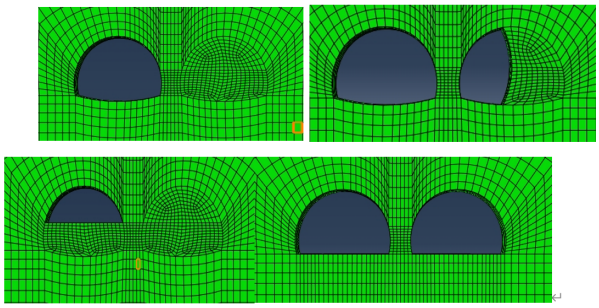

Figure 4. Construction Process Diagram for Class IV Rock Surrounds

sequence is shown in Figure 5.

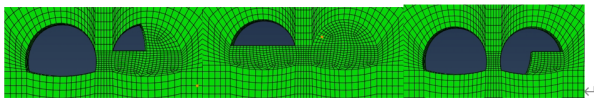

Figure 5. Construction Process Diagram for Class V Rock Surround

2.5. Characteristics of the Stress Field in the Surrounding Rock After Tunnel Excavation

1. **Maximum Principal Stresses**
   Figure 6 to 9 show the maximum principal stresses after excavation of the tunnels for Class II to Class V rock, respectively.

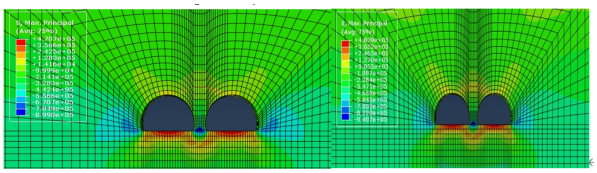

Figure 6. Distribution of Maximum Principal Stresses in the Class II Surrounding

From Figure 6 to 9, the maximum principal stress distribution in the surrounding rock after tunnel excavation shows that the tensile stresses in the Class II surrounding rock are concentrated at the bottom and top of the tunnel, with a maximum tensile stress of 0.48MPa, located at the bottom of the tunnel; the tensile stresses in the Class III surrounding rock are concentrated at the bottom and top of the tunnel, with a maximum tensile stress of 0.45MPa, occurring at the bottom of the tunnel; the tensile stresses in the Class IV surrounding rock are concentrated at the bottom and top of the tunnel, with a maximum tensile stress of is 0.13MPa; tensile stresses are concentrated above the rock column in Class V, with a maximum tensile stress of 0.12MPa.

2. **Minimum Principal Stresses**
   Figure 10 and 11 show the minimum principal stress distribution after excavation for small spaced tunnels from Class II to Class V surrounding rocks respectively.
   As can be seen from Figure 10 to 11, the minimum principal stresses in the surrounding rocks after tunnel excavation are concentrated in the rock column and on both sides of the tunnel, with a maximum compressive stress of 0.95 MPa at the bottom of the rock column. The maximum compressive stress is 0.52 MPa; the compressive stress concentration occurs near the rock column and the sides of the tunnel in Class V rock, with a maximum compressive stress of 0.33 MPa, occurring near the sides of the tunnel.

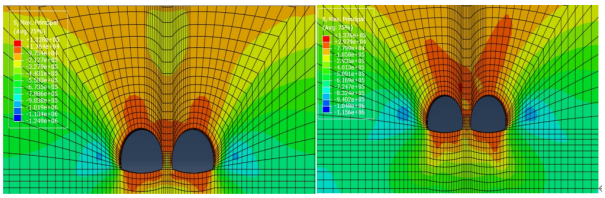

Figure 7. Distribution of Maximum Principal Stresses in the Class III Surrounding Rock

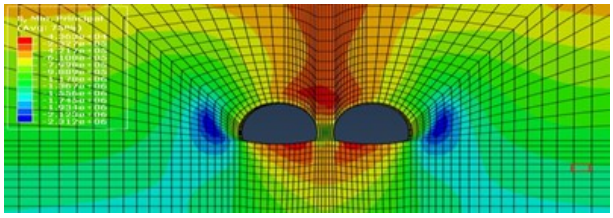

Figure 8. Distribution of Maximum Principal Stresses in the Class IV Surrounding Rock

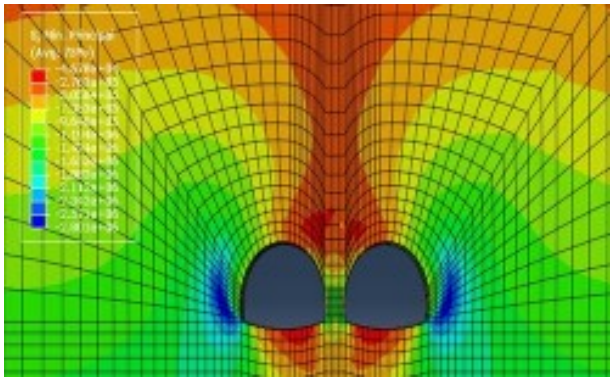

Figure 9. Distribution of Maximum Principal Stresses in the Class V Surrounding Rock

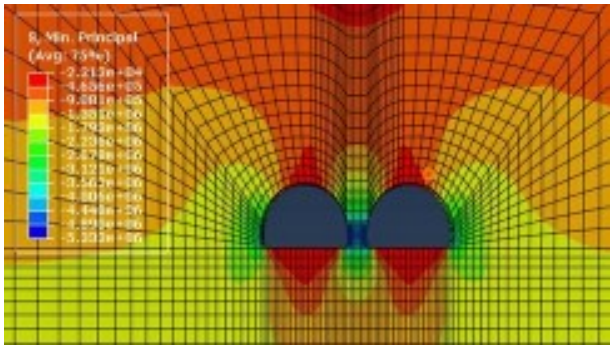

Figure 10. Distribution of Minimum Principal Stresses in Class II Enclosing Rocks

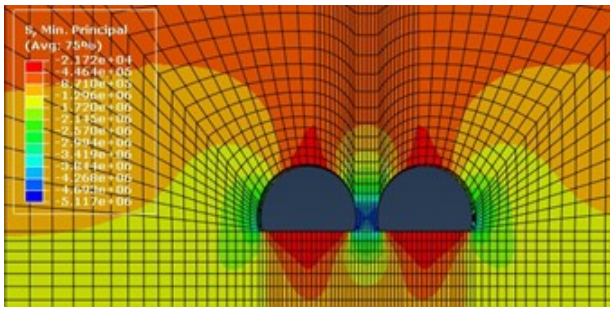

Figure 11. Distribution of Minimum Principal Stresses in Class III Enclosing Rocks

3. Property Identification Model for Rock Quality Classification

The problem of differentiating the quality of a rock mass by means of multiple indicators can be summarised as a comprehensive evaluation problem: let X be the evaluation object space, and its object x_i (i= 1,2,... ,n) has m evaluated indicators I_j (j= 1,2,... ,m). For each indicator I_j measurement t_j of x_i , there are p evaluation levels C_k (k= 1,2,... ,p), so that the level of t_j can be determined and the x_i can be evaluated together to determine its level.

The attribute identification model for comprehensive evaluation of rock quality classification consists of three aspects: single-indicator attribute measurement; multi-indicator integrated attribute measurement; attribute identification.

3.1. Single Indicator Attribute Measures

The size of the evaluated object x_i with level C_k is represented by the attribute measure $\mu_{xk} = \mu_{x_i} \in C_k$, and the size of the jth indicator value t_j of x_i with level C_k is represented by the attribute measure $\mu_{xk} = \mu_{t_j} \in C_k$. $\mu_{xk} = \mu_{t_j} \in C_k$ is determined by establishing its attribute measure function to represent the change in the attribute measure μ_{t_j} due to a change in t_j.

Determine the single-indicator attribute measure function $\mu_{xk}(t)$ as follows:

$$\mu_{xk}(t) = \begin{cases} 1 & t < a_{j1} - d_j, \\ \frac{a_{j1}+d_j-t}{2d_j} & a_{j1} - d_j \le t \le a_{j1} + d_j, \\ 0 & a_{j1} + d_j < t, \end{cases} \tag{6}$$

where, $j = 1, 2, ..., m; k = 2, 3, ..., p - 1$.

3.2. Multi-indicator Composite Attribute Measure

Single indicator attribute measures are weighted and summed to obtain a composite attribute measure u_{xk}:

$$u_{xk} = \sum_{j=1}^{m} \omega_k k, \tag{7}$$

where ω_j is the weight of the jth indicator I_j, satisfying:

$$\omega_j \geqslant 0, \quad \sum_{j=1}^{m} \omega_j = 1. \tag{8}$$

3.3. Property Identification

Confidence criterion: Let the evaluation set ($C_1, C_2, \cdots, C_K$) be an ordered set and satisfy $C_1 > C_2 > \cdots > C_K$, λ is the confidence level, which can be $0.5 < \lambda \leqslant 1$. If

$$k_0 = \mathrm{m\,in}\{\, k : \sum_{1\neq 1}^{\mathrm{k}} \mu_{\mathrm{xk}} \geqslant \lambda 1 \leqslant k \leqslant p\}, \tag{9}$$

then x is considered to belong to class Ck_0.

There are m evaluation indicators, which may or may not have the same importance. In this paper, we use the similarity number to define the similarity weight to give an objective weight to the evaluation indicators [18], in order to avoid the subjective preference brought by the expert assignment. The method and steps are as follows:

Assume that the weight values of each evaluation index are equal:

$$\omega_j = 1/m, \tag{10}$$

$$\mu_{ck} = \frac{1}{m} \sum_{j \neq k}^{m} \mu_{jk}\ , \tag{11}$$

where, $i = 1, 2, ..., n$; $j = 1, 2, ..., m$; $k = 1, 2, ..., p$.

4. Example of Rock Quality Assessment

4.1. Evaluation Indicators, Grading Criteria and Attribute Measurement Functions

In order to verify the validity and feasibility of the property identification model, a comparative analysis was carried out with the evaluation example of reference [19], and the data are shown in Table 2. With reference to the relevant research results, the comprehensive evaluation indexes of rock quality classification were determined as rock quality index RQD (%), uniaxial compressive strength (in MPa), joint spacing (in m), friction coefficient of joint surface f, the amount of groundwater infiltration Q in L (min-10m)] or the unit water absorption rate Q (in Lu). For excavated tunnels, it is convenient to use the measured seepage volume "L min" per 10m section of tunnel as the Q value. However, the size of the hole has a great impact on the amount of groundwater seepage, and there are obvious differences in the amount of groundwater seepage in different seasons, so using this to measure the quality of the rock seems to be somewhat imprecise, and the standard is not uniform. In water conservancy and hydropower projects, the results of borehole exploration are often used to judge the quality of the rock, especially in riverbed dams where drilling is much easier than exploring holes, even in underground plants, water transfer tunnels, diversion caverns and flood relief caverns, etc. In the process of site selection, drilling is often done first and then digging [20]. Therefore, the "water absorption rate per unit Q(Lu)" commonly used in water conservancy and hydropower engineering borehole exploration is more widespread. 1Lu=1L (min-MPa-m) means that under the action of 1MPa water pressure, in 1min, each 1m long borehole is absorbed by the rock body of 1L (litre) of water. It has nothing to do with the diameter of the tunnel and is very little affected by the season, so it is reasonable to use it to measure the quality of the rock, and there is a more uniform standard. It is therefore recommended to promote the use of the unit of water absorption rate Lu; in tunnels that have been excavated, if there are no conditions to do borehole pressure tests, we have to use the approximate unit of groundwater seepage L (min-10m). There is currently no conversion between the two, but they are roughly equivalent in terms of magnitude when used to describe the quality of the rock mass, so it is worth borrowing them for the time being and using the same quantitative scale. With reference to domestic and international experience in evaluating rock quality, rock stability is divided into five categories: Class I is stable, Class II is basically stable, Class III is poorly stable, Class IV is unstable, and Class V is extremely unstable. The relationships between the rock quality classes and the evaluation indicators are shown in Table 3.

Sample number	RQD/%	R_c /Mpa	J_1 /m	f	Q/Lu
A	86	96.44	2.12	0.97	12
B	65	76.54	0.33	0.65	11
C	83	112.15	1.8	0.7	10
D	40	57.19	0.25	0.45	12
E	78	108.63	1.76	0.67	5

Table 2. Sample Rock Quality Assessment

Sample number	RQD/%	R_c /Mpa	J_1 /m	f	Q/Lu
Sample number	Stable	Basically stable	Poor stability	Instable	Extremely unstable
RQD/%	100-90	90-75	75-50	50-25	<25
R_c /Mpa	300-200	200-100	100-50	50-25	<25
J_1 /m	5-3	3-1	1-0.3	0.3-0.05	<0.05
f	12-0.8	0.8-0.6	0.6-0.4	0.4-0.2	<0.2
Q/Lu	0-5	5-10	10-25	25-125	125-300

Table 3. Rock Quality Evaluation Indicators and Grading Criteria

4.2. Evaluation Methods and Steps

In step 1, we calculate the single indicator attribute measure. Based on the sample data in Table 2, the single-indicator attribute measures were calculated according to the single-indicator attribute measure function given in Table 4. According to Eq. (11), at this point $\mu_{ck} = \frac{1}{5}\sum_{j\neq k}^{m}\mu_{jk}$, the attribute measure matrix $\mu_{5\times5}$ was obtained as:

$$\mu_{5\times5} = \begin{bmatrix} 0 & 204 & 0 & 488 & 0 & 308 & 0 & 0 \\ 0 & 0 & 243 & 0 & 757 & 0 & 0 & 0 \\ 0 & 073 & 0 & 823 & 0 & 104 & 0 & 0 \\ 0 & 0 & 020 & 0 & 493 & 0 & 487 & 0 \\ 0 & 107 & 0 & 732 & 0 & 161 & 0 & 0 \end{bmatrix} \tag{12}$$

In the second step, the weights of each indicator I_j were determined ω_j . According to Eq. (11) and Eq. (12), we get: similarity coefficient r_j = (0.327,0.373,0.488,0.360,0.326), similarity weight ω_j = (0.174,0.199,0.260,0.192,0.174).

Finally in step 3, we Calculate the composite attribute measure and attribute identification. The composite attribute measure is calculated according to Eq. (11) μ_{xk} and formed into a composite attribute measure matrix $\mu_{5\times5}$.

$$\mu_{5\times5} = \begin{bmatrix} 0 & 185 & 0 & 530 & 0 & 284 & 0 & 0 \\ 0 & 0 & 225 & 0 & 775 & 0 & 0 & \\ 0 & 064 & 0 & 845 & 0 & 091 & 0 & 0 \\ 0 & 0 & 017 & 0 & 463 & 0 & 520 & 0 \\ 0 & 093 & 0 & 717 & 0 & 190 & 0 & 0 \end{bmatrix} \tag{13}$$

Taking λ= 0.6, attribute identification was performed according to Eq. (13), and the comprehensive evaluation results of each sample were obtained.

5. Analysis of Orthogonal Numerical Simulation Test Results

5.1. Analysis of the Results of the Horizontal Convergence Volume

The six factors affecting the amount of horizontal convergence and the amount of horizontal convergence were subjected to ANOVA and the results were calculated as shown in Table 4.

As can be seen in Table 4, the F-statistic for the horizontal convergence model is 35.348 with a probability level P-value of 0.000, which shows that this ANOVA is highly significant. The different magnitudes of the F-values for each factor indicate that each factor has a different degree of influence on the level of convergence.

Factor	Sum of squares of variance	Freedom	Mean square	F value	P
Correction model	1832.454	12	152.704	35.348	0
Modulus of elasticity	521.092	2	260.546	60.311	0
Poisson's ratio	59.043	0	29.521	6.834	0.037
Internal friction angle	480.403	2	345.720	80.027	0
Cohesion	691.144	2	345.720	80.027	0
Tensile strength	74.436	2	37.218	8.615	0.024
Density	60.4	2	3.02	0.699	0.54
Error	21.6	5	4.32	-	-
Total	20878.906	18	-	-	-

Table 4. Variance Analysis of Horizontal Convergence

5.2. Analysis of Results for the Amount of Vault Subsidence

The six factors affecting the amount of sinking in the vault and the amount of sinking were subjected to ANOVA and the results were calculated as shown in Table 5.

Factor	Sum of squares of variance	Freedom	Mean square	F value	P
Correction model	5617.281	12	468.106	39.941	0.001
Modulus of elasticity	703.174	2	351.589	25.497	0.002
Poisson's ratio	129.007	2	64.509	75.957	0.007
Internal friction angle	2444.642	2	1222.321	88.633	0.001
Cohesion	228.912	2	114.457	8.298	0.025
Total	9191.968	25	-	-	-

Table 5. Variance Analysis of Crown Settlement

As can be seen from Table 5, the F-statistic for the model for the amount of vault subsidence is 39.941 with a probability level P-value of 0.001, which shows that this ANOVA is very significant. The different magnitudes of the F-values for each factor indicate that each factor has a different degree of influence on the amount of vault subsidence.

5.3. Analysis of Results for the Shaping Zone Factor

The six factors affecting the shaping zone factor and the shaping zone factor were subjected to ANOVA and the results were calculated as shown in Table 6.

Factor	Sum of squares of variance	Freedom	Mean square	F value	P
Correction model	30.457	12	2.521	16.524	0.002
Modulus of elasticity	0.627	2	0.314	2.027	0.233
Poisson's ratio	14.58	2	7.286	47.821	0.001
Internal friction angle	12.974	2	6.458	42.567	0.001
Cohesion	1.547	2	0.774	5.064	0.059
Tensile strength	0.761	5	0.151	-	-
Total	60.946	25	-	-	-

Table 6. Variance Analysis on the Factor of Plastic Zone

As can be seen in Table 6, the F-statistic for the plastic zone factor model is 16.524 with a probability level of 0.003, which shows that this ANOVA is highly significant. As the magnitude of the F-value for each factor varies, it indicates that each factor has a different degree of influence on the plastic zone factor. The F-value of each factor was used to determine the magnitude of its influence.

5.4. Analysis of the Results of the Intuitive Analysis Chart

In order to analyse the influence of each factor on the horizontal convergence, vault subsidence and plastic zone factor of the tunnel more intuitively, the statistical results in the ANOVA of the horizontal convergence, vault subsidence and plastic zone factor were used to plot the influence curves of each factor on the horizontal convergence, vault subsidence and plastic zone factor, respectively, using the level of each factor as the horizontal coordinate and the corresponding mean as the vertical coordinate, as shown in Figure 12.

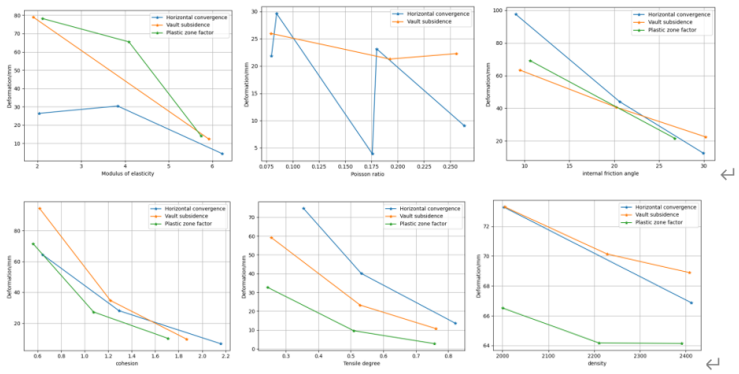

Figure 12. Influence of Various Factors on Horizontal Convergence, Crown Settlement and Factor of Plastic Zone

As can be seen from Figure 12 and the above analysis, the modulus of elasticity, Poisson's ratio, angle of internal friction, cohesion and tensile strength all have an influence on the horizontal convergence, vault subsidence and plastic zone factor of the tunnel, but to different degrees.

5.5. Analysis of Test Results for Varying Each Parameter

The changes in the horizontal convergence, vault subsidence and plastic zone factors of the tunnel envelope after changing any of the six factors are shown in Figure 13.

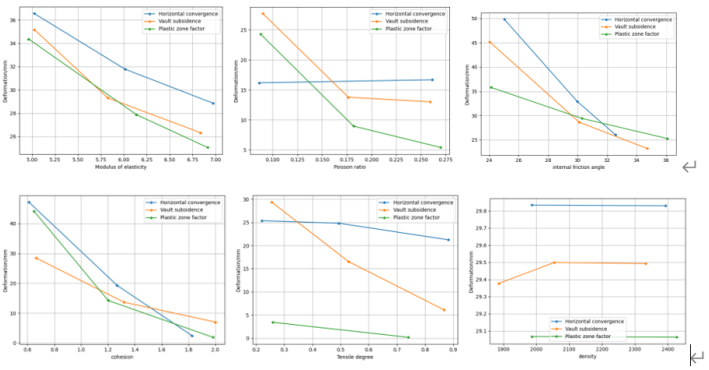

Figure 13. Curves of Horizontal Convergence, Crown Settlement and Factor of Plastic Zone of Tunnel After Change of Any Factor

Figure 13 shows that when only the modulus of elasticity, angle of internal friction, cohesion and tensile strength are varied, the horizontal convergence, vault subsidence and plastic zone factor all decrease as the values of these four factors increase. The stability of the surrounding rock is the ability of the surrounding rock not to deform after excavation of an underground chamber such as a tunnel. Consideration of the stability of the tunnel envelope should take into account the amount of horizontal convergence, the amount of vault subsidence and the plastic zone factor after excavation of the tunnel.

6. Conclusion

The study adopted the Mohr-Coulomb strength damage criterion for assessing rock mass behavior during tunnel excavation. Engineering mechanics parameters were determined based on rock physical and mechanical properties, facilitating numerical simulation of excavation processes. Various excavation methods were employed according to rock stability classification, with stress field characteristics analyzed post-excavation. A property identification model was proposed for rock quality classification, integrating single and multi-indicator measures. An example assessment demonstrated the model's application in evaluating rock stability.

Funding Statement

This study received the following funding support: Suzhou University, Suzhou City, Anhui Province Project Fund Number: 2023BSK071.

References

1. Su, Y., Su, Y., Zhao, M. and Vlachopoulos, N., 2021. Tunnel stability analysis in weak rocks using the convergence confinement method. *Rock Mechanics and Rock Engineering, 54*, pp.559-582.
2. Zhang, B., Ma, Z., Wang, X., Zhang, J. and Peng, W., 2020. Reliability analysis of anti-seismic stability of 3D pressurized tunnel faces by response surfaces method. *Geomechanics and Engineering, 20*(1), pp.43-54.
3. Xue, Y., Li, X., Li, G., Qiu, D., Gong, H., and Kong, F., 2020. An analytical model for assessing soft rock tunnel collapse risk and its engineering application. *Geomechanics and Engineering, 23*(5), pp.441-454.
4. Gholizadeh, H., Behrouj Peely, A., Karney, B. W., and Malekpour, A., 2020. Assessment of groundwater ingress to a partially pressurized water-conveyance tunnel using a conduit-flow process model: a case study in Iran. *Hydrogeology Journal, 28*(7), pp.2573-2585.
5. Frenelus, W., Peng, H., and Zhang, J., 2021. Evaluation methods for groundwater inflows into rock tunnels: a state-of-the-art review. *Int J Hydro, 5*(4), pp.152-168.
6. Huang, C. F., Zhang, S. L., Wu, S. C., and Gao, Y. T., 2022. Research and application of a comprehensive forecasting system for tunnels in water-bearing fault fracture zones: a case study. *Arabian Journal of Geosciences, 15*(2), pp.1-16
7. An, P., Wang, Z., and Zhang, C., 2022. Ensemble unsupervised autoencoders and Gaussian mixture model for cyberattack detection. Information Processing Management, 59(2), pp.102844.
8. Zhang, W., Zhang, R., Wu, C., Goh, A. T. C., Lacasse, S., Liu, Z., and Liu, H., 2020. State-of-the-art review of soft computing applications in underground excavations. *Geoscience Frontiers, 11*(4), pp.1095-1106.
9. Koopialipoor, M., Fahimifar, A., Ghaleini, E. N., Momenzadeh, M., and Armaghani, D. J., 2020. Development of a new hybrid ANN for solving a geotechnical problem related to tunnel boring machine performance. *Engineering with Computers, 36*(1), pp.345-357.
10. Zhou, J., Qiu, Y., Zhu, S., Armaghani, D.J., Li, C., Nguyen, H. and Yagiz, S., 2021. Optimization of support vector machine through the use of metaheuristic algorithms in forecasting TBM advance rate. *Engineering Applications of Artificial Intelligence, 97*, p.104015.
11. Bai, J., Wang, S., Xu, Q., Luo, Z., Zhang, Z., Lai, K.,and Wu, J., 2023. Intelligent real-time predicting method for rock characterization based on multi-source information integration while drilling. *Bulletin of Engineering Geology and the Environment, 82*(4), pp.150.

12. Huang, R., Liu, B., Sun, J., Song, Y., Yu, M., and Deng, T., 2024. Risk assessment approach for tunnel collapse based on improved multi-source evidence information fusion. *Environmental Earth Sciences, 83*(1), pp.18.

13. Pan, Y., Xia, Y., Li, Y., Yang, M., and Zhu, Q., 2023. Research on stability analysis of large karst cave structure based on multi-source point clouds modeling. *Earth Science Informatics, 16*(2), pp.1637-1656.

14. Zhang, L., Chao, W., Liu, Z., Cong, Y., and Wang, Z., 2022. Crack propagation characteristics during progressive failure of circular tunnels and the early warning thereof based on multi-sensor data fusion. *Geomechanics and Geophysics for Geo-Energy and Geo-Resources, 8*(5), p.172.

15. Wu, B., Qiu, W., Huang, W., Meng, G., Huang, J. and Xu, S., 2022. A multi-source information fusion approach in tunnel collapse risk analysis based on improved Dempster–Shafer evidence theory. *Scientific Reports, 12*(1), p.3626.

16. Xiao, D., Zhang, T., Zhou, X., Zheng, G., and Song, H., 2020. Safety monitoring of expressway construction based on multisource data fusion. *Journal of Advanced Transportation, 2020*, 1-11.

17. Wang, F., Yin, S., Guo, A., Wang, Z., Mi, M., Qi, G., Ma, J. and Zhang, H., 2021. Frame structure and engineering applications of the multisource system cloud service platform of monitoring of the soft rock tunnel. *Geofluids, 2021,* pp.1-15.

18. Li, B., Wang, E., Shang, Z., Liu, X., Li, Z., Li, B., Wang, H., Niu, Y. and Song, Y., 2021. Optimize the early warning time of coal and gas outburst by multi-source information fusion method during the tunneling process. *Process Safety and Environmental Protection, 149,* pp.839-849.

19. Xie, X., Zhang, D.M., Huang, H.W., Zhou, M.L., Lacasse, S. and Liu, Z.Q., 2021. Data fusion–based dynamic diagnosis for structural defects of shield tunnel. ASCE-ASME *Journal of Risk and Uncertainty in Engineering Systems, Part A: Civil Engineering, 7*(2), p.04021019.

20. Pan, Y., Xia, Y., Li, Y., Yang, M. and Zhu, Q., 2023. Research on stability analysis of large karst cave structure based on multi-source point clouds modeling. *Earth Science Informatics, 16*(2), pp.1637-1656.